

## Article

# Validation of the Physical and Mechanical Properties of *Eucalyptus benthamii* Maiden & Cambage Wood and Cross Laminated Timber Panels Using the Finite Element Method

Matheus Zanghelini Teixeira <sup>1,\*</sup>, Rodrigo Figueiredo Terezo <sup>2</sup>, Alexandro Bayestorff da Cunha <sup>2</sup>, Gustavo Faggiani Tomio <sup>2</sup>, Hector Bovo Coelho <sup>2</sup> and Camila Alves Corrêa <sup>2</sup>

- <sup>1</sup> Civil Engineering Department, Center for Optimization and Reliability in Engineering (CORE), Federal University of Santa Catarina (UFSC), Rua João Pio Duarte Silva, Florianópolis 88040-970, SC, Brazil
- <sup>2</sup> Forestry Engineering Department, Center for Agroveterinary Sciences (CAV), State University of Santa Catarina (UDESC), Av. Luiz de Camões, 2090, Conta Dinheiro, Lages 88520-000, SC, Brazil; rodrigo.terezo@udesc.br (R.F.T.); alexsandro.cunha@udesc.br (A.B.d.C.); ca.correa@edu.udesc.br (C.A.C.)
- \* Correspondence: matheus.zt@posgrad.ufsc.br

**Abstract:** Cross Laminated Timber (CLT) is a structurally complex panel that poses challenges in analysis due to the anisotropic nature of wood and the orthotropic characteristics of the composite. Numerical modeling using the Finite Element Method (FEM) offers a viable solution for analysis, particularly for addressing boundary value problems that are analytically challenging. Therefore, it is crucial to validate the experimental properties to ensure accurate results. The objective of this study was to validate the physical and mechanical properties for structural modeling using FEM, based on the characterization of *Eucalyptus benthamii* Maiden & Cambage wood and CLT panels. For wood characterization, the basic and apparent density were determined, and mechanical tests, including static bending, parallel-to-grain compression, and shear tests, were conducted. Utilizing the same batch of wood, three-layer CLT panels were manufactured and subjected to a non-destructive three-point bending test. This test was simulated in RFEM finite element software, employing Mindlin's theory, and the displacements obtained were compared with the experimental method. The results from a Student's *t*-test at a 5% significance level indicated no significant difference between the experimental and numerical methods, suggesting that the properties of the experimental *E. benthamii* CLT panel can be accurately represented by FEM.

**Keywords:** timber structures; numerical simulation; deflection; wood characterization



**Citation:** Teixeira, M.Z.; Terezo, R.F.; da Cunha, A.B.; Tomio, G.F.; Coelho, H.B.; Corrêa, C.A. Validation of the Physical and Mechanical Properties of *Eucalyptus benthamii* Maiden & Cambage Wood and Cross Laminated Timber Panels Using the Finite Element Method. *Forests* **2024**, *15*, 881. <https://doi.org/10.3390/f15050881>

Academic Editors: Zeki Candan and Mehmet Hakki Alma

Received: 7 April 2024  
Revised: 7 May 2024  
Accepted: 14 May 2024  
Published: 19 May 2024



**Copyright:** © 2024 by the authors. Licensee MDPI, Basel, Switzerland. This article is an open access article distributed under the terms and conditions of the Creative Commons Attribution (CC BY) license (<https://creativecommons.org/licenses/by/4.0/>).

## 1. Introduction

In the past two decades, there has been a notable surge in the utilization of timber structures in residential and commercial constructions. This trend is evident even in regions without a historical tradition of using this material. The significant progress can be attributed to the introduction of environmentally friendly and highly efficient wood products, such as Glued Laminated Timber (Glulam), Cross Laminated Timber (CLT) panels, and Laminated Veneer Lumber (LVL) panels. These components have found extensive applications in both unidirectional and bidirectional structures [1].

The construction method of CLT relies on self-supporting solid wood panels that serve as walls or slabs, streamlining the construction process for large or multi-story buildings and diverging from the constraints of traditional light wood construction systems. Typically, a CLT panel comprises layers of wood glued perpendicular to each other. With the advancements in the CLT panel industry, particularly in Europe, researchers and construction engineering professionals have shown keen interest in this product due to several associated benefits. These include a low environmental impact; a high strength-to-weight ratio; the ease and reduced time of installation; aesthetic appeal; lower carbon

dioxide emissions compared to steel and concrete structures; lower energy consumption in manufacturing; and increased resistance to fire, earthquakes, and heat [2].

When compared to solid wood, the cross-lamination of CLT layers allows for bidirectional load distribution and provides better dimensional stability and increased strength and rigidity, both within and outside the plane. This enables the manufacturing of wall panels and slabs with large dimensions, capable of spanning significant spans [3].

In Brazil, there are two CLT manufacturers: one located in the state of Paraná, in the south region, and the other in the state of São Paulo, in the southeast region. Both utilize wood from planted forests as their raw material. According to the Brazilian Tree Industry [4], Brazil ranks among the world's top 10 producers of sawn wood, with a total area of planted trees of 9.94 million hectares, consisting of 76% eucalyptus and 19% pine. This demonstrates the country's significant potential for CLT construction growth.

For the development of projects involving timber structures, a thorough understanding of the physical and mechanical properties of the selected wood is essential. These properties, typically determined through laboratory tests, serve as crucial inputs for analytical calculations during the design phase. However, the structural behavior of CLT panels, with their orthogonal characteristics, poses challenges for analytical calculations, as noted by Christovasilis et al. [5].

An alternative for understanding the structural behavior of more complex or anisotropic materials is the Finite Element Method (FEM). Unlike the analytical method, which provides exact solutions, solving a specific boundary value problem with FEM involves dividing the continuous material into small fragments, forming a mesh of finite elements. FEM provides numerical solutions that approximate exact solutions only at discrete points, which are the intersection points of the lines forming the finite elements, called nodes. The complete solution is generated by connecting the solutions of each element, allowing continuity between them [6]. It is important to carefully size this mesh so that the generated results are as reliable as possible.

To ensure reliable results through FEM, it is crucial for numerical models to accurately mirror real-world conditions. Therefore, the validation of properties becomes paramount, achieved through the numerical simulation of conducted tests. Research indicates the feasibility of validating properties and studying the structural behavior of CLT panels via FEM, as demonstrated in the study by Shirmohammadli et al. [7]. They developed models to assess rod connections in CLT, numerically simulating experiments and successfully validating them based on criteria such as the maximum load, displacement, and failure mode.

In a study by Zhang et al. [8], six Cross-Laminated Bamboo and Timber (CLBT) panels and two CLT panels were manufactured. They conducted a four-point bending test and compared the experimental flexural stiffness with the stiffness determined from the maximum load and displacement obtained through FEM simulation. Conclusively, they found that the numerical method was more accurate than the theoretical method, with a mean relative error within 10% between the experimental and simulated values for flexural stiffness. Another study by Akter et al. [9] successfully validated the properties of tests on two numerical models via FEM to ensure reliable results regarding the stiffness and strength of CLT wall–floor connections. One model resulted in a 6.9% mean absolute error and the other in a 4.9% mean absolute error, effectively representing the experimental data.

This research focuses on exploring the potential of *Eucalyptus benthamii* Maiden & Cambage wood, a species with rapid growth potential in Southern Brazil, particularly due to its resistance to harsh, cold conditions [10]. Several researchers have studied this species to understand its capabilities, as demonstrated in the studies by Silva et al., Tomio et al., Benin et al., Cunha et al., Müller et al., and Alves et al. [11–16]. However, none of the authors investigated *E. benthamii* as a raw material for CLT panels.

Therefore, the objective of this research was to validate the physical and mechanical properties in structural modeling via the FEM, based on the characterization of wood and CLT panels made from *Eucalyptus benthamii*.

## 2. Materials and Methods

### 2.1. Origin of the Wood

The *E. benthamii* wood used in this study originated from five trees in an experimental plantation, 23 years old, located at the Experimental Station of the Agricultural Research and Rural Extension Company of Santa Catarina (EPAGRI) in Lages, Santa Catarina, Brazil, located at latitude 27°48'20.9" S, longitude 50°20'10.8" W. The Lages region experiences an annual rainfall ranging between 1300 and 1500 mm, with an average temperature of 15 to 16 °C and a Köppen Cfb classification.

Experimental planting commenced in 1994 with the objective of observing species growth and adaptation to the local climate to potentially harvest seeds. Given the recent introduction of this species into the country, no defined rotation cycle has been established yet. Thirty trees were planted at a spacing of 3 × 3 m<sup>2</sup> in 5 rows, each row containing 6 trees. The soil at the site is characterized as acidic dystrophic, with only 200 g of NPK (50-20-10) fertilizer applied per hole before seed insertion.

The trees included in this study were randomly selected from the plantation, with an average height of 37.16 m and an average diameter at breast height (DBH) of 49 cm. The tree characteristics are detailed in Table 1.

**Table 1.** Characteristics of the trees.

Individuals	HT (m)	HC (m)	DBH (m)	CBH (m)
1	35.30	32.30	0.63	1.99
2	36.52	33.00	0.43	1.36
3	36.50	30.30	0.42	1.31
4	38.20	33.60	0.44	1.39
5	39.30	27.60	0.55	1.73
Mean	37.16	31.36	0.49	1.56

Legend: HT—torso height; HC—commercial height; DBH: diameter at breast height; CBH—circumference at breast height.

From each tree, the first log measuring 130 cm in length was extracted for wood characterization. A 5 cm thick disk was removed from the diameter at breast height (DBH) to determine the basic density. Subsequently, the second log, measuring 240 cm in length, was extracted to obtain lamellae for the experimental CLT production.

A 7 cm thick central plank was then cut from the first log of each tree using a simple band saw. This plank was further divided into pieces with a cross-section of 7 × 7 cm<sup>2</sup>, excluding the pith, using a multiple circular saw. These pieces were then utilized to create the test specimens. The second log was split tangentially with a simple band saw into 1-inch thick planks. These planks were subsequently sectioned with a multiple circular saw into 14 cm wide pieces of sawn timber. These pieces were naturally dried and utilized in CLT production. Figure 1 illustrates the log cutting scheme and wood extraction process.

### 2.2. Determination of the Physical and Mechanical Properties of Wood

From the pieces with a cross-section of 7 × 7 cm<sup>2</sup>, 30 specimens were prepared for various tests. These included 30 specimens for determining the apparent density according to COPANT 674 [17], with dimensions of 100 × 25 × 25 mm<sup>3</sup>; 30 specimens for the static bending test according to COPANT 555 [18], with dimensions of 300 × 20 × 20 mm<sup>3</sup>; 30 specimens for the compression test parallel to the fibers according to COPANT 464 [19], with dimensions of 200 × 50 × 50 mm<sup>3</sup>; and 30 specimens for the shear test according to COPANT 463 [20], with dimensions of 65 × 50 × 50 mm<sup>3</sup>. Prior to conducting the tests, the specimens were stored in a climate-controlled environment with a temperature of 20 ± 3 °C and relative humidity of 65 ± 5% until mass stabilization [21]. An exception was made for the disks, which underwent saturation and drying at 103 ± 2 °C for the subsequent determination of the basic density according to COPANT 461 [22].

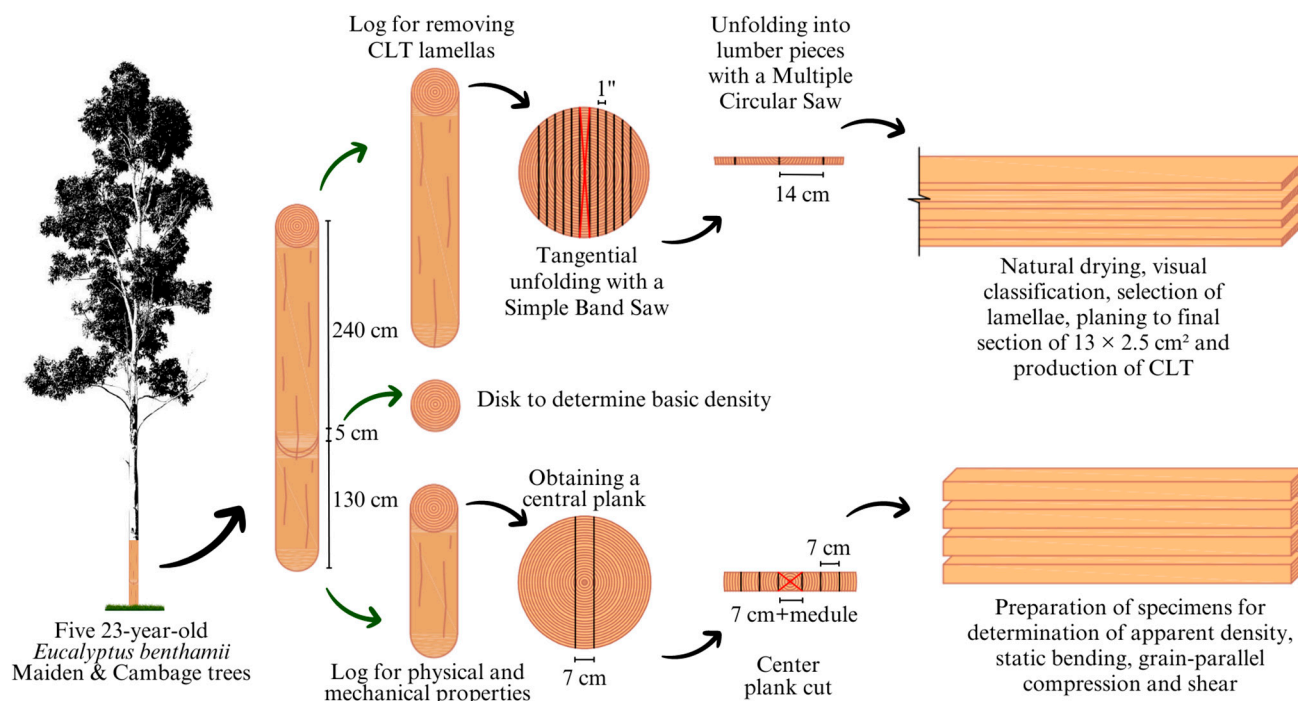


**Figure 1.** Log cutting scheme and wood extraction process. The red cross marks indicate the sections of the wood containing pith, which were not used.

### 2.3. Experimental Production of CLT

Three CLT panels with three layers of *E. benthamii* wood were produced. The panel production process followed these steps: (I) visual classification of sawn wood pieces from the splitting of the second logs and natural drying, according to ABNT NBR 14806 [23] and ABNT NBR 11700 [24]; (II) selection of defect-free lamellae (30) of first-class quality for the outer layers of the panels, and selection of second-class quality lamellae (30), which only had firm knot defects, for the intermediate layers of the CLT; (III) trimming to standardize the width of the pieces to 130 mm; (IV) planing to calibrate the pieces to approximately 25 mm; (V) end trimming of the pieces from the outer layers and pieces from the central layer, with no finger joints on any piece; (VI) the application of polyurethane adhesive (PUR) with a weight of 200 g/m<sup>2</sup> in a single line; (VII) assembling the panels in a crosswise manner; (VIII) pressing at room temperature for 24 h under a pressure of 0.6 MPa; (IX) squaring to regulate the edges; and (X) conditioning until a constant mass, i.e., until reaching 12% moisture content. The final dimensions of the panels, after squaring, are listed in Table 2.

**Table 2.** Dimensions of the CLT panels.

CLT Panel	Total Thickness (mm)	Length (mm)	Width (mm)
1	75	2040	650
2	76	2100	660
3	77	2100	655

### 2.4. Non-Destructive Static Bending Tests on the CLT Panels

The non-destructive three-point static bending test was conducted following the layout described ABNT NBR 7190 [25], as depicted in Figure 2. A Charlott manual hydraulic press with a load capacity of 100 tons and a U10M/5 kN load cell equipped with WA 50 mm displacement transducers were utilized to perform the test. Displacement measurements were obtained using an inductive transducer (WA<sup>®</sup> 50 mm) coupled with a data

acquisition system (Quantum-X<sup>®</sup>) and software (Catman Easy<sup>®</sup>, version 1.9.0) from HBM<sup>®</sup> (Darmstadt, Germany).

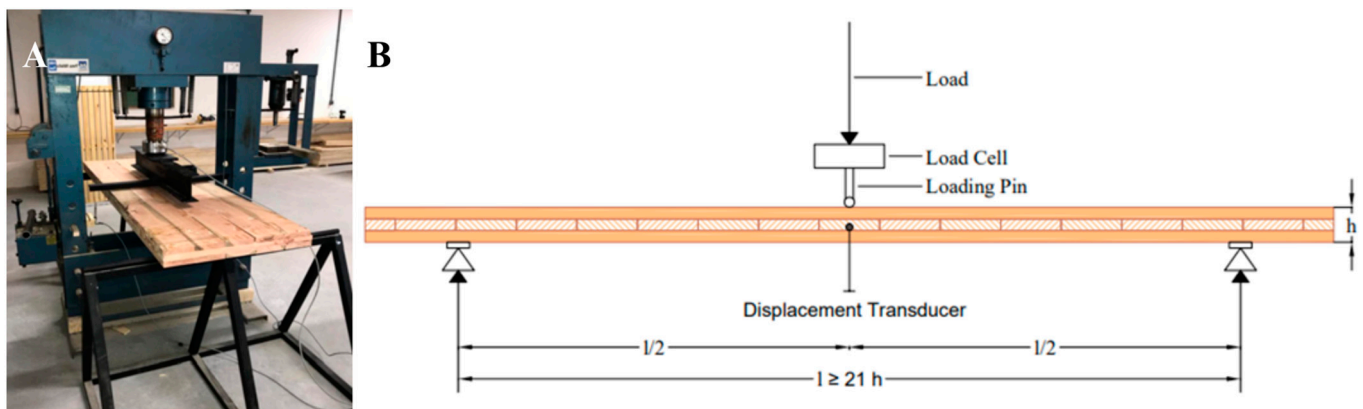


**Figure 2.** (A) Three-point bending test experiment, and (B) 3-point panel bending test layout.

Each panel was tested twice: once on the (A) top face, and then, it was flipped over and tested on the (B) bottom face. The span between supports was standardized at 1680 mm for all three panels, adhering to the minimum span requirement of 21 times the thickness of the CLT ( $21h$ ) established by the standard. A loading rate of 10 MPa/min was applied, with two loading and unloading cycles, adhering to the minimum threshold of 10% and maximum threshold of 50% of the estimated breaking load value. Subsequently, loading was applied up to the elastic limit of each panel. The estimated breaking value was obtained from the solid wood bending test ( $f_M$ ), which was also utilized for the FEM modeling.

This test was simulated in finite element software, using the same load application data to obtain the corresponding vertical displacements. The goal was to compare the experimental method with the numerical method, facilitating the validation of the wood properties.

### 2.5. Numerical Simulation of CLT and Validation of Wood Properties

A structural numerical modeling of CLT panels was performed using the FEM in RFEM<sup>®</sup> software from Dlubal<sup>®</sup> (Tiefenbach, Germany), version 5.26, and its additional module RF-Laminate<sup>®</sup>, allowing the configuration of surfaces as laminated and orthotropic elements. The software was calculated using the Mindlin theory, recommended for thicker plates such as CLT, as it considers the shear strain effect throughout the thickness.

To simulate the experimental three-point bending test, structural modeling followed the same experimental conditions, adhering to the dimensions of the CLT panels and the same span between articulated supports. Six simulations were conducted, corresponding to two tests per CLT panel—one on side A and the other on side B.

In the software, the finite element mesh consisted of quadrangles, with carefully defined dimensions to ensure results faithful to the real model. Various mesh element sizes (100 cm, 40 cm, 10 cm, and 2 cm) were tested to achieve the optimal refinement. It was found that the displacement results remained consistent with elements smaller than 40 cm. Generally, a finer mesh tends to yield more accurate results, hence the selection of a 2 cm mesh (Figure 3).

After defining the mesh, the physical and mechanical properties obtained from the solid wood tests were incorporated into the layers of the CLT panels. Additionally, RF-Laminate<sup>®</sup> was supplied with other properties, such as Poisson's ratio  $\nu_{xy}$ , suggested by Bodig and Jayne [26] with a value of 0.37 for dicotyledons, and the stiffness moduli. For the latter, the same authors recommended specific relationships based on the flexural modulus of elasticity:

$$E_x : E_y : E_z \simeq 20 : 1.6 : 1 \quad (1)$$

$$G_{xy} : G_{xz} : G_{yz} \simeq 10 : 9.4 : 1 \quad (2)$$

$$E_x : G_{xy} \simeq 14 : 1 \quad (3)$$

As for the mechanical properties of strength and stiffness, additional values that were not experimentally estimated are required. Brazilian standards do not provide some of these values, so European standards were sought, where the CLT system is already well established. The EN 16351 [27] standard of the European Committee for Standardization (CEN) proposes a value for shear strength by rolling ( $f_R$ ) of 1.10 MPa for panels where the side surfaces of the boards are not glued together, which is the case in this study. The tensile strength perpendicular to the grain ( $f_{t90}$ ) was estimated using the BS EN 338 [28] standard of the British Standards Institution (BSI) and the NBR 7190-1 [29] standard of the Brazilian Association of Technical Standards (ABNT), considering the value of 0.60 MPa for hardwoods. The other values, such as the compression strength perpendicular to the grain ( $f_{c90}$ ) and tensile strength parallel to the grain ( $f_{t0}$ ), followed the estimation calculations determined by ABNT NBR 7190-3 [30].

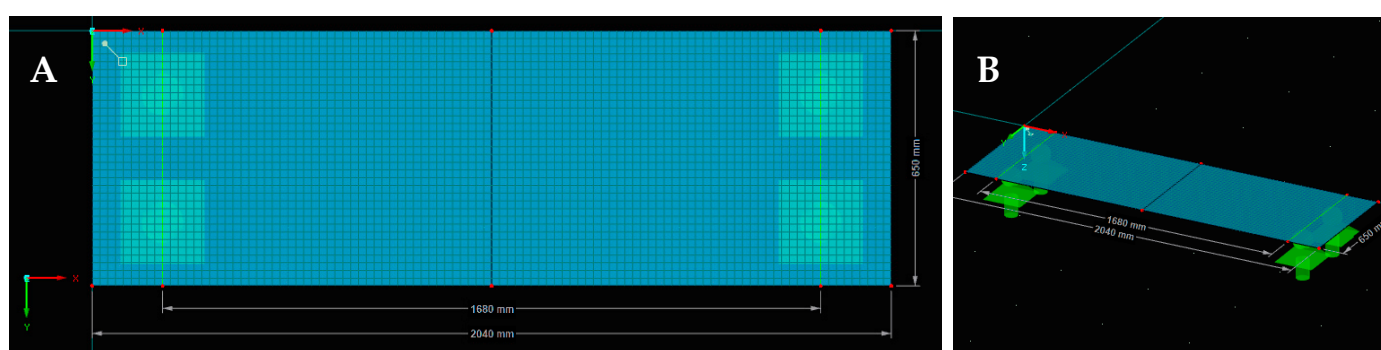


**Figure 3.** FE model with the 2 cm mesh applied (CLT Panel 1). (A) Top view and (B) perspective.

In addition to defining and inputting the properties into the software, the coupling between the layers was considered to simulate bonding between the larger faces of the panels. The modeling also accounted for the lamellas' width of 130 mm and the absence of glue on their side edges. Since the sides of the lamellas were not glued, CEN Eurocode 5 [31] specifies a torsional stiffness reduction factor of  $K_{33} = 0.489$  and a layer  $K_{88} = 0.585$ .

### 2.6. Data Analysis

The normality of the vertical displacement data obtained in the three-point bending test was assessed using a Quantile–Quantile plot (Q–Q Plot). The comparison of these values between the experimental and numerical methods was conducted using the independent samples  $t$ -test in R<sup>®</sup> software, version 4.1.1, with a 95% confidence level.

## 3. Results and Discussion

### 3.1. Physical and Mechanical Properties of Wood

The results obtained for the apparent and basic density of 23-year-old *E. benthamii* wood are presented in Table 3, showing average values of 740 kg/m<sup>3</sup> and 610 kg/m<sup>3</sup>, respectively. According to Hillis [32], this classifies it as a moderately heavy mature wood [33].

**Table 3.** Density of *Eucalyptus benthamii* Maiden & Cambage wood and comparison values.

Species	Age (Years)	Origin	Reference	Density (kg/m <sup>3</sup> )	
				Basic ( $\rho$ )	12%
<i>E. benthamii</i>	23	Lages-SC		610	740
Minimum density value				540	650
Maximum density value			---	660	870

Table 3. Cont.

Species	Age (Years)	Origin	Reference	Density (kg/m <sup>3</sup> )	
				Basic ( $\rho$ )	12%
Standard deviation				48.45	34.44
Coefficient of variation (%)				9.86	9.21
<i>Eucalyptus dunnii</i> Maiden	28	Pelotas-RS	Gallio et al. [34]	573	-
<i>Eucalyptus grandis</i> W. Hill ex Maiden	25	Telêmaco Borba-PR	Silva et al. [35]	420	550
<i>Eucalyptus saligna</i> Sm.	23	Piracicaba-SP	Bortoletto Júnior [36]	560	-
<i>Eucalyptus urophylla</i> S. T. Blake	21	Piracicaba-SP	Bortoletto Júnior [36]	600	-
<i>E. dunnii</i>	16	Colombo-PR	Severo & Tomaselli [37]	573	-
<i>E. grandis</i>	17	Martinho Campos-MG	Gonçalez et al. [38]	590	-
<i>E. benthamii</i>	13	Palmeira-SC	Nones et al. [39]	505	684
<i>E. benthamii</i>	11	Guatambu-SC	Gallio et al. [40]	548	-
<i>E. dunnii</i>	11	Telêmaco Borba-PR	Batista et al. [41]	560	-
<i>E. benthamii</i>	7	Colombo-SC	Pereira et al. [42]	477	-
<i>E. benthamii</i>	6	Cerro Negro-SC	Müller et al. [15]	520	610
<i>E. benthamii</i>	6	Guarapuava-PR	Benin et al. [13]	500	-

It can be inferred that there was a superiority in the density of *E. benthamii* wood in this study when compared to other species of similar age and with a shorter rotation cycle, especially with *Eucalyptus dunnii* Maiden, which also thrives in environments with intense cold and frost occurrences. The coefficients of variation found were low, 9.86% and 9.21%, which were lower than those proposed by Green et al. [43] for species of the *Eucalyptus* spp. genus, demonstrating little variation among the evaluated trees.

The variations in density among and within species are attributed to differences in the wood's anatomical structure, such as cell wall thickness, size and quantity of different cell types, and changes in the chemical components. These variations are primarily derived from tree age, genotype, site index, climate, geographical location, and silvicultural practices. Despite understanding that density is a key property defining wood quality due to its various correlations with others, it should not be considered the sole parameter for decision-making in terms of behavior in processes and final use.

Regarding the results of the mechanical properties of *E. benthamii* wood, they are expressed as average values in Table 4. In general, 23-year-old *E. benthamii* showed higher values for all properties compared to species of the same genus and the same species at younger ages, except for the static flexural modulus of elasticity of 17-year-old *Eucalyptus grandis* W. Hill ex Maiden wood, as determined by Gonçalez et al. [38], and 16-year-old *E. dunnii* wood, assessed by Severo & Tomaselli [44].

Table 4. Mechanical properties of *E. benthamii* wood and comparison values.

Species	Age (Years)	Origin	Reference	SB (MPa)		PC (MPa)		SH (MPa) ( $f_v$ )
				MOR ( $f_M$ )	MOE ( $E_x$ )	MOR ( $f_{c0}$ )	MOE ( $E_{c0}$ )	
<i>E. benthamii</i>	23	Lages	---	109.11	15,325.48	43.51	12,212.29	13.07
Minimum value				96.63	13,842.61	35.44	12,152.92	10.83
Maximum value				125.07	16,108.97	49.45	12,293.07	14.33
Standard deviation				15.51	720.77	6.16	51.41	0.84
Coefficient of variation (%)				14.21	9.79	11.18	6.78	6.26
<i>E. grandis</i>	25	Telêmaco Borba	Silva et al. [45]	85.22	12,803.67	---	---	---
<i>E. grandis</i>	17	Martinho Campos	Gonçalez et al. [38]	84.14	15,647.84	---	---	---
<i>E. dunnii</i>	16	Colombo	Severo & Tomaselli [44]	103.17	17,828.77	---	---	---
<i>E. grandis</i>	15	Viçosa	Lobão et al. [46]	76.35	15,275.00	55.90	19,137.00	10.20
<i>E. grandis</i> × <i>E. urophylla</i>	13	Mucuri	Gonçaves et al. [47]	103.20	12,474.00	---	---	---

Table 4. Cont.

Species	Age (Years)	Origin	Reference	SB (MPa)		PC (MPa)		SH (MPa) ( $f_v$ )
				MOR ( $f_M$ )	MOE ( $E_x$ )	MOR ( $f_{c0}$ )	MOE ( $E_{c0}$ )	
<i>E. urophylla</i>	11	Vazante	Cruz et al. [48]	79.00	12,527.00	40.00	6590	----
<i>E. benthamii</i>	6	Cerro Negro	Müller et al. [15]	83.53	9754.67	37.34	2565.00	11.41
<i>E. benthamii</i>	6	Guarapuava	Benin et al. [13]	74.00	8330.00	31.23	4621.19	11.90

Legend: SB—static bending; PC—parallel compression; SH—shear; MOR—modulus of rupture; MOE—modulus of elasticity;  $f_M$ —static bending strength;  $E_x$ —modulus of elasticity obtained in the static bending test;  $f_{c0}$ —compressive strength parallel to the grain;  $E_{c0}$ —modulus of elasticity in compression parallel to the grain;  $f_v$ —shear strength.

The stiffness and strength of wood, along with density, tend to increase with the age of the tree due to the thickening of the cell walls and a reduction in cell width [49]. According to Moura and Brito [50], as the tree ages and the growth rate decreases, more cellulose macromolecules accumulate in the secondary walls of the fibers. Consequently, the cell walls become thicker, potentially resulting in higher resistance values.

In the static bending test, crucial for determining the load-bearing capacity in the structural components [47], the *E. benthamii* wood in this study exhibited MOE and MOR values superior to those of species from the same genus that are already used for structural purposes. Therefore, the use of this 23-year-old species for similar structural applications can be considered.

For parallel compression to the fibers, the 23-year-old *E. benthamii* also resulted in higher MOR and MOE values, except when compared to the 15-year-old *E. grandis* from the study by Lobão et al. [46]. This does not diminish its importance, as, for example, *E. benthamii* wood still has a higher resistance value than the specifications parallel to the mechanical property classes of NBR 7190-2 [51].

For the tangential shear, higher values were also observed compared to those mentioned in other studies, which, according to Moreschi [52], has a strong relationship with the wood density. One of the advantages of wood having good shear strength is, according to Müller et al. [15], its use as embedded structural elements.

### 3.2. Flexural Deflection of CLT and Validation of Properties through FEM

In each bending test, the maximum load applied in the elastic regime and its corresponding displacement were recorded. The same maximum loads applied to the experimental panels were used in the numerical simulation of the test to determine the displacement obtained by the FEM. With the experimental properties obtained from the wood, it was possible to estimate the rigidity moduli  $G$  in different planes, the compression perpendicular to the grain strength ( $f_{c90}$ ), and the tension parallel to the grain strength ( $f_{t0}$ ). The results of these parameters, along with all the others used in the modeling, are summarized in Table 5.

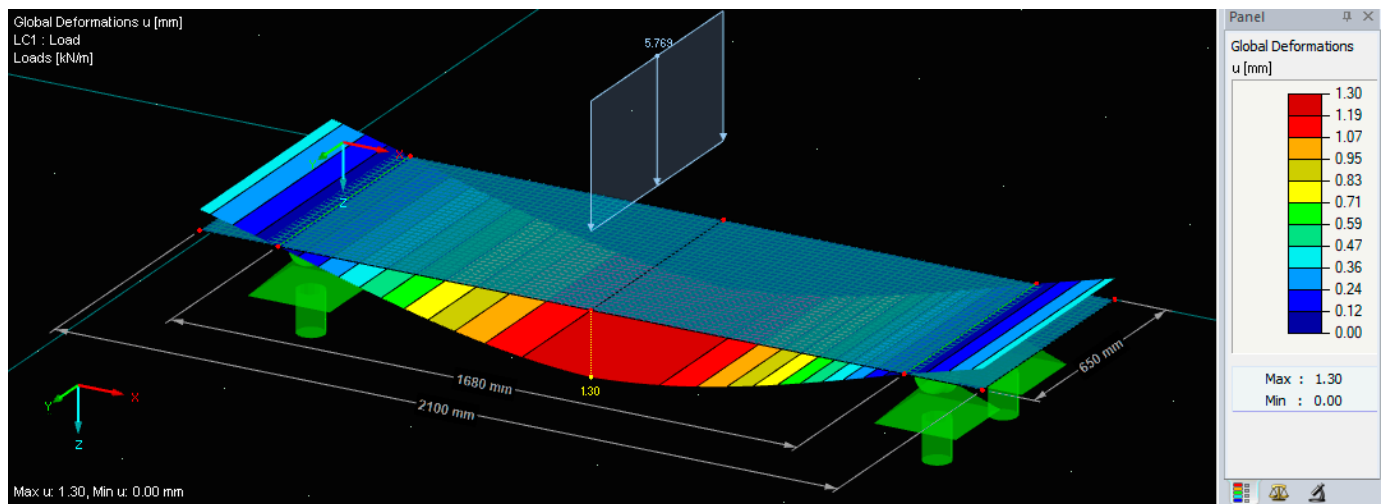
The structural numerical models in RFEM<sup>®</sup> displayed the vertical displacement results for each test. The software allowed for a graphical representation of the results, as shown in Figure 4. Table 6 presents the maximum loads applied to each panel and the displacement results in both the experimental method and the FEM.

Comparing the results, it is possible to observe high coefficients of variation in both methods but significantly higher in the experimental method (41.36%). One contributing factor to the high coefficients of variation is that the lamellas were not mechanically graded before composing the experimental panel, while, in the FEM, all panels used exactly the same average physical and mechanical properties of *E. benthamii* wood. The current NBR 7190-2 [51] recommends visual and mechanical grading for structural elements, and the choice of the resistance class is based on the lower classification between the two.

**Table 5.** FEM modeling parameters.

Normative and Literature Parameters				
$\nu_{xy}$	$f_R$ (MPa)	$f_{t90}$ (MPa)	K33	K88
0.37	1.10	0.60	0.489	0.585
Parameters Obtained Experimentally				
$\rho$ (kg/m <sup>3</sup> )	$f_M$	$E_x$	$f_{c0}$	$f_v$
610	109.11	15,325.48	43.51	13.07
Parameters Estimated with Experimental Results				
$f_{c90}$ (MPa)	$f_{t0}$ (MPa)	$G_{xz}$ (MPa)	$G_{yz}$ (MPa)	$G_{xy}$ (MPa)
10.88	56.51	1029.00	109.47	1094.68

Legend:  $\nu_{xy}$ —Poisson's ratio for the dicotyledons;  $f_R$ —shear strength by rolling;  $f_{t90}$ —tensile strength perpendicular to the grain;  $k33$ —torsional stiffness reduction factor;  $K88$ —layer stiffness reduction factor;  $\rho$ —basic density;  $f_M$ —static bending strength;  $E_x$ —modulus of elasticity obtained in the static bending test;  $f_{c0}$ —compressive strength parallel to the grain;  $f_v$ —shear strength;  $f_{c90}$ —compression perpendicular to the grain strength;  $f_{t0}$ —tensile strength parallel to the grain;  $G_{xz}$ —modulus of rigidity in the xz plane;  $G_{yz}$ —modulus of rigidity in the yz plane;  $G_{xy}$ —modulus of rigidity in the xy plane.

**Figure 4.** Deflection of CLT in the FE model of the three-point bending test.**Table 6.** Vertical displacements obtained in the three-point bending tests by the experimental method and FEM.

CLT Panel	Maximum Applied Load (kN)	Experimental Method (mm)	Finite Element Method (mm)	Difference between Methods (%)
1A	3.75	1.39	1.30	6.47
1B	5.76	1.86	2.00	7.00
2A	6.50	2.07	2.16	4.17
2B	6.90	2.96	2.29	22.64
3A	7.04	4.40	2.26	48.64
3B	5.81	3.14	1.86	40.76
Mean		2.64	1.98	21.61
Coefficient of variation (%)		41.36	18.70	

Furthermore, the difference between the experimental and finite element displacements ranged from 4.17% to 48.64%, with an average of 21.61%. This difference is similar to what was observed by Sciomenta et al. [53], who compared experimental deflection with FEM results from a four-point bending test on CLT panels composed of three layers. The panels were modeled in two configurations, one homogeneous and the other mixed, with

two types of wood in its composition. The authors showed there was a good relationship between the displacement results of the experimental and numerical methods, with a difference of 15% for homogeneous CLT and 22% for mixed CLT. These differences may result from wood being an anisotropic and heterogeneous material, which also implies the possibility of defects present inside the elements that were not visible on their exterior.

Table 5 also shows that the average displacements obtained by the numerical model were lower than the displacements from the experimental test. The same behavior was observed by Wang et al. [54], who produced three- and four-layer CLT with visually graded wood and tested them in an experimental concentrated load rupture test to assess the bending properties. The authors simulated the test using FEM with a 5 cm mesh and obtained a modeled average deflection smaller than the measured deflection in the experimental test. They emphasized that this was due to the fact that defects present in the wood were not included in the model and that there may be errors in handling real experiments while FE models are fed by the average properties. However, the difference between the displacements of the two methods was not significant, meaning they obtained consistent results, showing confidence in the validation.

The results of the statistical analysis to check the normality of the data are shown in Figure 5. It can be observed that there is linearity in the Q–Q plot graph, although each method presents a discrepant value on the upper edge (experimental method) and the lower edge (numerical method). After confirming the normality of the data, a Student's *t*-test was performed with a 5% significance level, which yielded a *p*-value of 0.2099. For a *p*-value greater than 0.05,  $H_0$  is accepted, which is the hypothesis that there is no statistically significant difference between the methods.

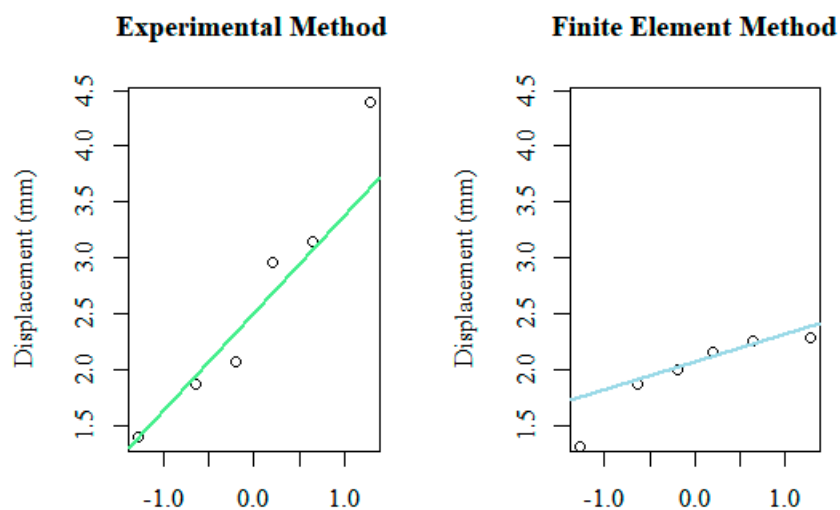


Figure 5. Normality test by Q–Q Plot.

#### 4. Conclusions

The 23-year-old *E. benthamii* wood from Southern Brazil exhibited average density values indicative of maturity and moderate weight. The research conducted demonstrated that its physical and mechanical properties either matched or surpassed those of younger woods of the same species and woods of the same genus in the studies cited. The deflection obtained in the experimental three-point bending tests of the three-layer *E. benthamii* CLT was compared with simulations using the FEM. The difference between the methods was 21.61%, statistically insignificant, according to the Student's *t*-test at the 5% significance level. This validates the wood properties, indicating that experimental CLT made from *E. benthamii* can be accurately represented by FEM. The research paves the way for future Finite Element Modeling studies to evaluate the performance of these panels as floor, ceiling, and wall slabs in sustainable construction projects.

**Author Contributions:** Conceptualization, M.Z.T. and R.F.T.; methodology, R.F.T. and A.B.d.C.; software, M.Z.T.; validation, M.Z.T. and R.F.T.; formal analysis, M.Z.T.; investigation, G.F.T. and H.B.C.; writing—original draft preparation, M.Z.T., G.F.T. and H.B.C.; writing—review and editing, M.Z.T., A.B.d.C. and C.A.C.; visualization, C.A.C.; supervision, R.F.T. and A.B.d.C.; project administration, R.F.T. All authors have read and agreed to the published version of the manuscript.

**Funding:** This research was funded by the State Fund for the Maintenance and Development of Higher Education Fund (FUMDES/UNIEDU), Public Notice 261/SED/2022, the Foundation for Research and Innovation Support of the Santa Catarina State (FAPESC), PAP 01/2021, and the Graduate Monitoring Scholarship Program (PROMOP), Notice 01/2021, from the Santa Catarina State University (UDESC).

**Data Availability Statement:** The original contributions presented in the study are included in the article, further inquiries can be directed to the corresponding author.

**Acknowledgments:** The authors would like to express their sincere gratitude to the Agricultural Research and Rural Extension Company of Santa Catarina (EPAGRI) for providing the logs for this research.

**Conflicts of Interest:** The authors declare no conflicts of interest.

## References

- Sandoli, A.; D’Ambra, C.; Ceraldi, C.; Calderoni, B.; Prota, A. Sustainable Cross-Laminated Timber Structures in a Seismic Area: Overview and Future Trends. *Appl. Sci.* **2021**, *11*, 2078. [\[CrossRef\]](#)
- Younis, A.; Doodoo, A. Cross-laminated timber for building construction: A life-cycle-assessment overview. *J. Build. Eng.* **2022**, *52*, 104482. [\[CrossRef\]](#)
- Gagnon, S.; Karacabeyli, E. *CLT Handbook Canadian Edition*; FPInnovation: Port-Claire, QC, Canada, 2019.
- Indústria Brasileira de Árvores (IBÁ). *Relatório IBÁ 2023*; IBÁ: São Paulo, Brazil, 2023.
- Christovasilis, I.; Brunetti, M.; Follasa, M.; Nocetti, M.; Vassalo, D. Evaluation of the mechanical properties of cross laminated timber with elementary beam theories. *Constr. Build. Mater.* **2016**, *122*, 202–213. [\[CrossRef\]](#)
- Moaveni, S. *Finite Element Analysis: Theory and Application with ANSYS*; Prentice Hall: Upper Saddle River, NJ, USA, 1999.
- Shirmohammadli, Y.; Hashemi, A.; Masoudnia, R.; Quenneville, P. Numerical modeling investigation of cross-laminated timber connections consisting of multiple glued-in rods. *Structures* **2023**, *53*, 491–500. [\[CrossRef\]](#)
- Zhang, X.; Yang, S.; Fei, B.; Qin, D.; Yang, J.; Li, H.; Wang, X. Bending and shear performance of a cross-laminated composite consisting of flattened bamboo board and Chinese fir lumber. *Constr. Build. Mater.* **2023**, *392*, 131913. [\[CrossRef\]](#)
- Akter, S.T.; Schweigler, M.; Serrano, E.; Bader, T.K. A Numerical Study of the Stiffness and Strength of Cross-Laminated Timber Wall-to-Floor Connections under Compression Perpendicular to the Grain. *Buildings* **2021**, *11*, 442. [\[CrossRef\]](#)
- Silva, L.D.; Higa, A.R.; Santos, G.A. Desafios do uso da madeira de *Eucalyptus benthamii* para serraria. In *Silvicultura e Melhoramento Genético de Eucalyptus Benthamii*; Editora FUPEF: Curitiba, Brazil, 2012; pp. 123–150.
- Silva, L.D.; Higa, A.R.; Floss, P.A.; Croce, D.M.; Resende, M.D.V.; Garcia, J.N.; Spiecker, H.; Khale, H. *Eucalyptus benthamii*: Uma espécie geneticamente promissora para produção de madeira em áreas sujeitas a ocorrência de geadas. *Rev. Floresta* **2022**, *52*, 422–435. [\[CrossRef\]](#)
- Tomio, G.F.; Cunha, A.B.; Brand, M.A.; Córdova, U.A. Rendimento e qualidade da madeira de *Eucalyptus benthamii* Maiden et Cambage de rotação longa no processo de desdobro. *Sci. For.* **2021**, *49*, e3689. [\[CrossRef\]](#)
- Benin, C.C.; Watzlawick, L.F.; Hillig, E. Propriedades físicas e mecânicas da madeira de *Eucalyptus benthamii* sob efeito do espaçamento de plantio. *Ciência Florest.* **2017**, *27*, 1375–1384. [\[CrossRef\]](#)
- Cunha, A.B.; Brand, M.A.; Simão, R.L.; Martins, S.A.; Anjos, R.A.M.; Surdi, P.G.; Schimalski, M.B. Determinação do rendimento de matéria-prima de *Eucalyptus benthamii* Maiden & Cambage por meio de diferentes métodos de desdobro. *Rev. Árvore* **2015**, *39*, 733–741.
- Müller, B.V.; Rocha, M.P.; Cunha, A.B.; Klitzke, R.J.; Nicoletti, M.F. Avaliação das principais propriedades físicas e mecânicas da madeira de *Eucalyptus benthamii* Maiden et Cambage. *Floresta Ambiente* **2014**, *21*, 535–542. [\[CrossRef\]](#)
- Alves, I.C.N.; Gomide, J.L.; Colodette, J.L.; Silva, H.D. Caracterização tecnológica da madeira de *Eucalyptus benthamii* para produção de celulose kraft. *Ciência Florest.* **2011**, *21*, 167–174. [\[CrossRef\]](#)
- COPANT 674; Método de Determinación del Peso Específico Aparente. Comisión Panamericana de Normas Técnicas—COPANT: Ciudad de Guatemala, Guatemala, 1972.
- COPANT 555; Flexão Estática. Comisión Panamericana de Normas Técnicas—COPANT: Ciudad de Guatemala, Guatemala, 1972.
- COPANT 464; Compressão Paralela às Fibras. Comisión Panamericana de Normas Técnicas—COPANT: Ciudad de Guatemala, Guatemala, 1972.
- COPANT 463; Cisalhamento. Comisión Panamericana de Normas Técnicas—COPANT: Ciudad de Guatemala, Guatemala, 1972.
- COPANT 459; Acondicionamento dos Corpos-de-Prova. Comisión Panamericana de Normas Técnicas—COPANT: Ciudad de Guatemala, Guatemala, 1972.

22. COPANT 461; Massa Específica Aparente Básica. Comisión Panamericana de Normas Técnicas—COPANT: Ciudad de Guatemala, Guatemala, 1972.
23. NBR 14806; Madeira—Madeira Serrada de Eucalipto. Associação Brasileira de Normas Técnicas (ABNT): Rio de Janeiro, Brazil, 2002.
24. NBR 11700; Madeira Serrada de Coníferas Provenientes de Reflorestamento para uso Geral—Classificação. Associação Brasileira de Normas Técnicas (ABNT): Rio de Janeiro, Brazil, 1991.
25. NBR 7190; Projeto de Estruturas de Madeira. Associação Brasileira de Normas Técnicas (ABNT): Rio de Janeiro, Brazil, 1997.
26. Bodig, J.; Jayne, B.A. *Mechanics of Wood and Wood Composites*; Van Nostrand: New York, NY, USA, 1982.
27. EN 16351; Timber Structures—Cross Laminated Timber—Requirements. Comité Européen de Normalization (CEN): Brussels, Belgium, 2015.
28. BS EN 338; Structural Timber—Strength Classes. British Standards Institution (BSI): London, UK, 2016.
29. NBR 7190-1 Projeto de Estruturas de Madeira. Parte 1: Critérios de Dimensionamento, Associação Brasileira de Normas Técnicas (ABNT): Rio de Janeiro, Brazil, 2022.
30. NBR 7190-3; Projeto de Estruturas de Madeira. Parte 3: Métodos de Ensaio para Corpos de Prova Isentos de Defeitos para Madeiras de Florestas Nativas. Associação Brasileira de Normas Técnicas (ABNT): Rio de Janeiro, Brazil, 2022.
31. Eurocode 5; Design of Timber Structure. Part 1-1: General—Common Rules and Rules for Buildings. Comité Européen de Normalization (CEN): Brussels, Belgium, 2004.
32. Hillis, W.E. Wood quality and growing to meet market requirements. In *The Future of Eucalypts for Wood Products*; Proceedings; IUFRO: Launceston, Australia, 2000; pp. 256–264.
33. Mainieri, C.; Chimelo, J.P. *Fichas de Características das Madeiras Brasileiras*; IPT: São Paulo, Brazil, 1989; 418p.
34. Gallio, E.; Zanatta, P.; Machado, S.F.; Beltrame, R.; Gatto, D.A. Caracterização de propriedades tecnológicas de três folhosas deterioradas por térmitas. *Rev. Matéria* **2018**, *23*, e12239. [[CrossRef](#)]
35. Silva, J.C.; Oliveira, J.T.S.; Tomazello Filho, M.; Keinert Júnior, S.; Matos, J.L.M. Influência da idade e da posição radial na massa específica da madeira de *Eucalyptus grandis* Hill ex. Maiden. *Rev. Floresta* **2004**, *34*, 13–22. [[CrossRef](#)]
36. Bortoletto Júnior, G. Produção de compensados com 11 espécies do gênero *Eucalyptus*, avaliação das suas propriedades físico-mecânicas e indicações para utilização. *Sci. For.* **2003**, *63*, 65–78.
37. Severo, E.T.D.; Tomaselli, I. Efeito da pré-vaporização em algumas propriedades físicas da madeira de *Eucalyptus dunnii*. *Cerne* **2001**, *7*, 35–42.
38. Gonçalves, J.C.; Breda, L.C.S.; Barros, J.F.M.; Macedo, D.G.; Janin, G.; Costa, A.F.; Vale, A.T. Características tecnológicas das madeiras de *Eucalyptus grandis* W. Hill ex Maiden e *Eucalyptus cloeziana* F. Muell visando o seu aproveitamento na indústria moveleira. *Ciência Florest.* **2006**, *16*, 329–341. [[CrossRef](#)]
39. Nones, D.L.; Brand, M.A.; Cunha, A.B.; Carvalho, A.F.; Weise, S.M.K. Determinação das propriedades energéticas da madeira e do carvão vegetal produzido a partir de *Eucalyptus benthamii*. *Rev. Floresta* **2015**, *45*, 57–64. [[CrossRef](#)]
40. Gallio, E.; Santini, E.J.; Gatto, D.A.; De Souza, J.T.; Ravasi, R.; De Menezes, W.M.; Floss, P.A.; Beltrame, R. Caracterização Tecnológica da Madeira de *Eucalyptus benthamii* Maiden et Cambage. *Sci. Agrar. Parana.* **2016**, *15*, 244–250. [[CrossRef](#)]
41. Batista, D.C.; Klitzke, R.J.; Santos, C.V.T. Densidade básica e retratibilidade da madeira de clones de três espécies de *Eucalyptus*. *Ciência Florest.* **2010**, *20*, 665–674. [[CrossRef](#)]
42. Pereira, J.C.D.; Schaitza, E.G.; Shimizu, J.Y. *Características Físicas, Químicas e Rendimentos da Destilação seca da Madeira de Eucalyptus Benthamii Maiden et Cambage*; Embrapa Florestas: Colombo, Sri Lanka, 2001; 4p.
43. Green, D.W.; Winandy, J.E.; Kretschmann, D.E. Mechanical properties of wood. In *Forest Products Laboratory. Wood Handbook: Wood as an Engineering Material*; USDA: Washington, DC, USA, 1999.
44. Severo, E.T.D.; Tomaselli, I. Efeito do tratamento de vaporização em toras e madeira serrada de *Eucalyptus dunnii* sobre a flexão estática. *Rev. Floresta* **1999**, *29*, 37–51. [[CrossRef](#)]
45. Silva, J.C.; Matos, J.L.M.; Oliveira, J.T.S.; Evangelista, W.V. Influência da idade e da posição radial na flexão estática da madeira de *Eucalyptus grandis* Hill ex. Maiden. *Rev. Árvore* **2005**, *29*, 795–799. [[CrossRef](#)]
46. Lobão, M.S.; Lúcia, R.M.D.; Moreira, M.S.S.; Gomes, A. Caracterização das propriedades físico-mecânicas da madeira de eucalipto com diferentes densidades. *Rev. Árvore* **2004**, *28*, 889–894. [[CrossRef](#)]
47. Gonçalves, F.G.; Oliveira, J.T.S.; Della Lucia, R.M.; Sartorio, R.C. Estudo de algumas propriedades mecânicas da madeira de um híbrido clonal de *Eucalyptus urophylla* x *Eucalyptus grandis*. *Rev. Árvore* **2009**, *33*, 501–509. [[CrossRef](#)]
48. Cruz, C.R.; Lima, J.T.; Muniz, G.I.B. Variações dentro das árvores e entre clones das propriedades físicas e mecânicas da madeira de híbridos de *Eucalyptus*. *Sci. For.* **2003**, *64*, 33–47.
49. Vital, B.R. *Métodos de Determinação da Densidade da Madeira*; Sociedade de Investigações Florestais: Viçosa, Brazil, 1984; 21p.
50. Moura, L.F.; Brito, J.O. Influência da desrama artificial sobre a densidade básica, a composição química e as características dos traqueídeos da madeira de *Pinus caribaea* var. *hondurensis* Barr. et Golf. *Rev. Árvore* **2001**, *25*, 369–374.
51. NBR 7190-2; Projeto de Estruturas de Madeira. Parte 2: Métodos de Ensaio para Classificação Visual e Mecânica de Peças Estruturais de Madeira. Associação Brasileira de Normas Técnicas (ABNT): Rio de Janeiro, Brazil, 2022.
52. Moreschi, J.C. *Propriedades da Madeira*, 4th ed.; Departamento de Engenharia e Tecnologia Florestal, Setor de Ciências Agrárias/UFPR: Curitiba, Brazil, 2012.

- 
53. Sciomenta, M.; Egidio, A.D.; Bedon, C.; Fragiacomò, M. Linear model to describe the working of a three layers CLT strip slab: Experimental and numerical validation. *Adv. Struct. Eng.* **2021**, *24*, 3118–3132. [[CrossRef](#)]
  54. Wang, J.; Ning, F.; Li, J.; Zhu, H. Experimental study and finite element simulation analysis of the bending properties of Cross-Laminated Timber (CLT) two-way plates. *J. Eng. Sci. Technol. Rev.* **2020**, *13*, 132–142. [[CrossRef](#)]

**Disclaimer/Publisher’s Note:** The statements, opinions and data contained in all publications are solely those of the individual author(s) and contributor(s) and not of MDPI and/or the editor(s). MDPI and/or the editor(s) disclaim responsibility for any injury to people or property resulting from any ideas, methods, instructions or products referred to in the content.